THE JOURNAL OF BIOLOGICAL CHEMISTRY VOL. 285, NO. 1, pp. 493–501, January 1, 2010

Characterization of a Bifunctional Pyranose-Furanose Mutase from *Campylobacter jejuni* 11168*[S]

Received for publication, October 2, 2009, and in revised form, October 29, 2009 Published, JBC Papers in Press, November 3, 2009, DOI 10.1074/jbc.M109.072157

Myles B. Poulin[‡§1], Harald Nothaft[§¶], Isabelle Hug[§¶], Mario F. Feldman[§¶2], Christine M. Szymanski[§¶3], and Todd L. Lowary[‡§4]

From the Departments of [‡]Chemistry and [¶]Biological Sciences and the [§]Alberta Ingenuity Centre for Carbohydrate Science, University of Alberta, Edmonton, Alberta T6G 2R3, Canada

UDP-galactopyranose mutases (UGM) are the enzymes responsible for the synthesis of UDP-galactofuranose (UDP-Gal*f*) from UDP-galactopyranose (UDP-Gal*p*). The enzyme, encoded by the *glf* gene, is present in bacteria, parasites, and fungi that express Gal*f* in their glycoconjugates. Recently, a UGM homologue encoded by the *cj1439* gene has been identified in *Campylobacter jejuni* 11168, an organism possessing no Gal*f*-containing glycoconjugates. However, the capsular polysaccharide from this strain contains a 2-acetamido-2-deoxy-D-galactofuranose (Gal*f*NAc) moiety. Using an *in vitro* high performance liquid chromatography assay and complementation studies, we characterized the activity of this UGM homologue. The enzyme, which we have renamed UDP-*N*-acetylgalactopyranose mutase (UNGM), has relaxed specificity and can use either UDP-Gal or UDP-GalNAc as a substrate. Complementation studies of mutase knock-outs in *C. jejuni* 11168 and *Escherichia coli* W3110, the latter containing Gal*f* residues in its lipopolysaccharide, demonstrated that the enzyme recognizes both UDP-Gal and UDP-GalNAc *in vivo*. A homology model of UNGM and site-directed mutagenesis led to the identification of two active site amino acid residues involved in the recognition of the UDP-GalNAc substrate. The specificity of UNGM was characterized using a two-substrate co-incubation assay, which demonstrated, surprisingly, that UDP-Gal is a better substrate than UDP-GalNAc.

In nature, hexose sugars are found predominantly in the thermodynamically favored pyranose ring form; however, hexose sugars in the furanose ring form are found in bacteria, fungi, and parasites (1, 2). For example, D-galactofuranose (Gal*f*)[5] is a component in many microbial cell surface oligosaccharides (3, 4) and is a major structural component of the mycobacterial cell wall (5). In many pathogenic microorganisms, these Gal*f* residues are essential for cell viability or play a crucial role in cell physiology (6, 7). For this reason, and because hexofuranose sugars are absent in mammalian cell saccharide structures (1), there has been a surge of interest in studying and identifying inhibitors of Gal*f* biosynthesis (8).

The sugar nucleotide UDP-Gal*f* is the precursor of Gal*f* and is incorporated into growing oligosaccharides via galactofuranosyltransferase-mediated reactions (9). First identified in *Escherichia coli* (10), the enzyme UDP-D-galactopyranose mutase (UGM) is responsible for the biosynthesis of UDP-Gal*f* via the ring contraction of UDP-galactopyranose (UDP-Gal*p*). UGM is encoded by the *glf* gene for which homologues have since been identified in *Klebsiella pneumoniae* (11), mycobacterial species (12), and in various eukaryotic pathogens (13, 14). Since the advent of rapid genome sequencing, a number of putative UGMs have been identified throughout the microbial species; however, very few of the gene products have been confirmed by biochemical analysis.

UGM is a flavoprotein and catalyzes the reversible ring contraction of UDP-Gal*p* to UDP-Gal*f* via a unique mechanism (Fig. 1) (15). The noncovalently bound FAD co-factor is directly involved in catalysis and must be in the reduced form for the enzyme to be active (16). Because of the interest in UGM as a drug target (8), significant work has been done to study its mechanism, and it has been shown that the reduced $FADH^-$ acts as a nucleophile and displaces the anomeric UDP to form a covalent intermediate (17). Formation of an iminium ion breaks the O5–C1 bond of the galactose moiety leading to a covalently bound acyclic intermediate. This species can then cyclize to the furanose ring form.

Although the enzyme mechanism is generally understood, there are still many unanswered questions about the enzyme-substrate interactions. The UGM protein structure contains a mobile loop region, which adopts either an open or closed form in the crystal structures that have been determined to date (15, 18) with the closed structure being the catalytically active form. This loop has been shown to close upon substrate binding (19), and a conserved arginine (Arg-174 in *K. pneumoniae*, Arg-170 in *E. coli*, and Arg-180 in *Mycobacterium tuberculosis*) has been found to be essential for UGM activity (20). This arginine appears to stabilize the negatively charged diphosphate backbone of the sugar nucleotide substrate. Many synthetic analogues (21–26) have been used to probe the mechanism of UGM and investigate substrate binding, but until recently, no

* This work was supported in part by the Alberta Ingenuity Centre for Carbohydrate Science and National Sciences and Engineering Research Council of Canada.

[S] The on-line version of this article (available at http://www.jbc.org) contains supplemental Figs. S1–S2 and Tables S1–S2.

[1] Recipient of a studentship award from Alberta Ingenuity.

[2] Alberta Heritage Foundation for Medical Research Scholar.

[3] Alberta Ingenuity Scholar. To whom correspondence may be addressed. Tel.: 780-248-1234; Fax: 780-492-9234; E-mail: cszymans@ualberta.ca.

[4] To whom correspondence may be addressed. Tel.: 780-492-1861; Fax: 780-492-7705; E-mail: tlowary@ualberta.ca.

[5] The abbreviations used are: Gal*f*, D-galactofuranose; Cj, *Campylobacter jejuni*; CPS, capsular polysaccharide; Ec, *Escherichia coli*; LPS, lipopolysaccharide; UGM, UDP-galactopyranose mutase; UNGM, UDP-N-acetylgalactopyranose mutase; Gal*p*, galactopyranose; HPLC, high pressure liquid chromatography.

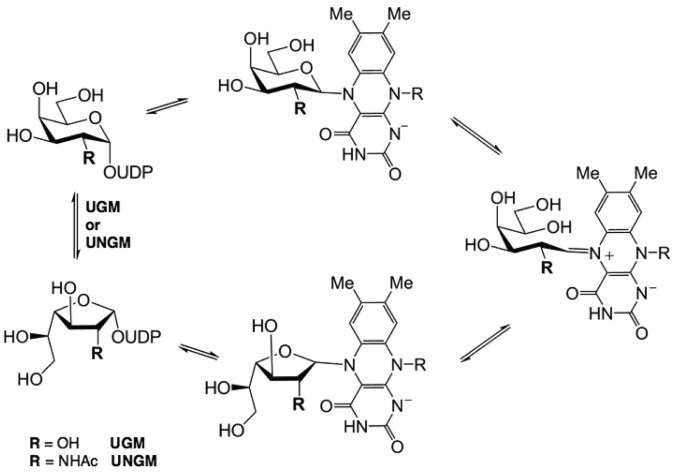

FIGURE 1. **UGM reaction mechanism.**

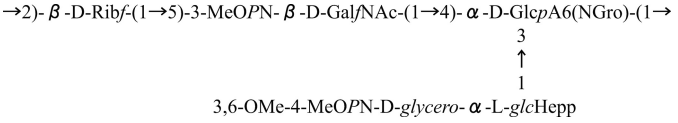

FIGURE 2. **Capsular polysaccharide structure of *C. jejuni* 11168.** Shown is the tetrasaccharide repeat unit of *C. jejuni* 11168 (HS:2 serotype) with the Gal*f*NAc residue shown in *boldface*.

ligand-bound crystal structures have been available. Tryptophan fluorescence (15) and molecular modeling have predicted that the uridine of the UDP-Gal base stacks with Trp-160 (numbering for *K. pneumoniae*) (27); in contrast, recent crystal structures of the *K. pneumoniae* UGM with bound UDP-Glc*p* (28) and UDP-Gal*p* (29) show that the uridine stacks against tyrosine 155 in the active site. This discrepancy demonstrates that many of the key binding interactions responsible for the substrate specificity of UGM still remain to be elucidated.

Although Gal*f* is the most common naturally occurring hexofuranose, it is not unique. 6-Deoxy-D-galactofuranose (30), 6-deoxy-L-altrofuranose (31), and 2-acetamido-2-deoxy-D-galactofuranose (32, 33), among others, have also been identified in bacterial saccharide structures. However, little is known about the biosynthesis of these other hexofuranose sugars. Previous work has established that the UGM from *K. pneumoniae*, which has been the most studied, is unable to catalyze the synthesis of either UDP-Fuc*f* or UDP-Gal*f*NAc (26, 34). Recently it has been shown that a homologue of the *glf* gene, *fcf2* in *E. coli* O52, acts as a Fuc*f* mutase enzyme for the biosynthesis of TDP-Fuc*f* (35). This protein has 60% identity to the *K. pneumoniae* UGM, but the origin of the difference in substrate tolerance is unknown.

The bacterium *Campylobacter jejuni* is a foodborne pathogen that is a leading cause of diarrheal disease worldwide (36). Infections by this organism have also been linked to the development of the neurological disorder Guillain-Barré syndrome (37). Previous work showed that the capsular polysaccharide (CPS) from the 11168 strain contains a Gal*f*NAc residue (Fig. 2) (33). *C. jejuni* 11168 also contains a homologue of the *glf* gene *cj1439*. Because no Gal*f* residues have been found in *C. jejuni* 11168 glycoconjugates, it has been proposed that the *cj1439* gene product is responsible for the biosynthesis of UDP-Gal*f*NAc from UDP-Gal*p*NAc (33). Herein, we report studies on the protein produced by expression of *cj1439* and demonstrate its activity as a UDP-*N*-acetylgalactopyranose mutase (UNGM). We also have demonstrated that the enzyme can use both UDP-Gal and UDP-GalNAc as substrates and have investigated the origins of this substrate selectivity using site-directed mutagenesis to identify key residues that allow for the turnover of UDP-GalNAc.

EXPERIMENTAL PROCEDURES

Preparation of UDP-sugars—UDP-Gal*p* and UDP-Gal*p*NAc were obtained from Aldrich and used without further purification. UDP-Gal*f* was prepared from synthetic Gal*f*-1-phosphate (38) using galactose-1-phosphate uridyltransferase and UDP-glucose pyrophosphorylase as described by Errey *et al.* (39). All stock solutions were prepared by dissolving the appropriate quantity of UDP-sugar in 100 mM potassium phosphate (pH 7.4). Before use, stock solutions were calibrated by HPLC co-injection with a known concentration of UDP.

Cloning, Expression, and Purification of Glf Proteins—For MFF1 (Ec-*glf* mutant) and Cj1439c (Cj-*glf* mutant) complementation and *in vivo* Glf analyses, *glf* alleles were put under the control of the constitutive *C. jejuni-E. coli* shuttle promoter replacing the *gfp* gene on plasmid pWM1007 (40). Cj-*glf* alleles were amplified by PCR using oligonucleotides CS261 and CS262 that introduce restriction sites for EcoRI and BsrGI, whereas Ec-*glf* was amplified with oligonucleotides CS362 and CS363 introducing an EcoRI site in the 5′ end of Ec-*glf*. For both species, a C-terminal His tag was introduced via PCR, where the plasmid pJHCV32 (41) and chromosomal DNA of *C. jejuni* 11168-V26 (42) served as template DNA, respectively. The EcoRI-BsrGI-digested Cj-*glf* PCR product was ligated with the purified 8643-bp pWM1007 vector DNA fragment obtained after digestion with the same enzymes. The Ec-*glf* PCR product, subsequently treated with T4 DNA polymerase and EcoRI, was inserted into the purified 8297-bp pWM1007 vector subsequently treated with SfuI, T4 DNA polymerase, and EcoRI. For expression in *C. jejuni,* the *kan* (kanamycin) cassette within the pWM1007-Cj-*glf* construct was replaced by the *cat* (chloramphenicol) cassette after EcoRV digestion of the vector and ligation with an 842-bp DNA fragment containing the *cat* cassette isolated from plasmid pRY109 (43) after SmaI digestion. A similar strategy was carried out for the pWM1007 Ec-*glf* constructs, except that the 8428-bp vector fragment was purified after partial digestion with EcoRV. Orientation of the *cat* gene on the resulting plasmids (same orientation as the nonpolar *kan* cassette) was verified by restriction analyses. For high yield expression of Ec-*glf*, the corresponding gene was amplified by PCR using oligonucleotides CS372 and CS373 to introduce NdeI and XhoI restriction sites, respectively. Plasmid pJHCV32 (41) served as template DNA for the PCR. After restriction digestion, the purified DNA fragment was ligated into plasmid pET22b cut with the same enzymes.

Expression of soluble C-terminal hexahistidine-tagged *E. coli* UGM protein from plasmid pET-Ec-*glf* in BL21 was observed after induction with 0.01 mM isopropyl β-D-1-thiogalactopyranoside for 2 h at room temperature (22 °C). C-terminal hexahistidine-tagged *C. jejuni* UNGM was expressed in

E. coli DH5α from plasmid pWM1007 (*kan*)-Cj-*glf* after growth for 18 h at 28 °C. Soluble UNGM-His_6 proteins were purified by nickel-nitrilotriacetic acid affinity chromatography as described previously.

UNGM Activity Assay—The activity of purified wild-type and mutant proteins was assayed by incubating a mixture of sugar nucleotide (UDP-Gal*p*, UDP-Gal*f*, UDP-Gal*p*NAc, or UDP-Gal*f*NAc, 1 mM) and mutase protein (3.9 μM) in 30 μl of 100 mM potassium phosphate buffer (pH 7.4) containing freshly prepared sodium dithionite (20 mM) for 2-, 5-, 10-, and 20-min periods at 37 °C. Reactions were monitored by HPLC (Varian Prostar 210) following conditions similar to those previously reported by Zhang and Liu (16). A C_{18} column (Microsorb-MV, Varian, 4.6 × 250 mm) was used, and elution was done with 50 mM triethylammonium acetate buffer (pH 6.5) containing 1.5% acetonitrile. A flow rate lower than that described earlier (0.6 ml/min) (16) was used to increase separation, and the UV detector was set to a wavelength of 262 nm. Base-line resolution for all substrates was achieved, and the retention times for UDP-Gal*p*, UDP-Gal*f*, UDP-Gal*p*NAc, and UDP-Gal*f*NAc were found to be 8.8, 10.6, 10.0, and 12.5 min, respectively. The amount of conversion was determined by integration of the product and starting material peaks.

Enzymatic Synthesis of UDP-GalfNAc (Compound 2)—To confirm the identity of the product of the UNGM incubation with UDP-Gal*p*NAc, a milligram scale reaction of UDP-Gal*f*NAc was carried out. UDP-Gal*p*NAc (1 mM, 25 mg) was incubated with 4.7 μM UNGM in 2 ml of 100 mM potassium phosphate buffer (pH 7.4) containing freshly prepared sodium dithionite (20 mM) for 1 h at 37 °C. Compound 2 was purified by HPLC using a C_{18} column (Microsorb, Varian, 21.4 × 250 mm). The eluent used was 50 mM triethylammonium acetate (pH 6.5) containing 1.5% acetonitrile at a flow rate of 7.0 ml/min. The retention time of compound 2 was 22.3 min under these conditions. The product was further purified by chromatography on a Sephadex G-15 column (21.4 × 250 mm) eluting with Milli Q H_2O. The product was lyophilized to obtain a white powder (1 mg, 4% yield). The ^1H NMR data for the product can be found in the supplemental Table S2. Negative ion high resolution electrospray ionization mass spectrometry *m/z* calculated for $C_{17}H_{25}N_3O_{17}P_2$ $[M - 2H]^{2-}$ was 302.5335 and found was 302.5339.

NMR Spectroscopy—NMR spectra were obtained at 27 °C using a Varian DirectDrive two-channel spectrometer operating at 499.822 MHz for ^1H. Samples were prepared at concentrations of ~1.5 mM in D_2O. Chemical shifts were externally referenced to 0.1% acetone signal (2.225 ppm). A sweep width of 6010 Hz was used for measurement of the one-dimensional ^1H NMR spectrum with a 3.0 s relaxation time. The free induction decay signal gave a final digital resolution of 0.1 Hz/point. All coupling constants are reported in hertz (see supplemental Table S2). A two-dimensional ^1H–^1H COSY spectrum of compound 2 (supplemental Fig. S1) was obtained using a 6010 Hz sweep width with a 1.0-s acquisition time, a 0.1 relaxation delay, and 426 t_1 increments.

Determination of the Pyranose-Furanose Distribution at Equilibrium—The distribution of pyranose to furanose ring forms was measured at equilibrium and determined by integration of the appropriate peaks from the HPLC. The ratio was determined for both UDP-Gal and UDP-GalNAc substrates in both the forward and reverse directions. For the forward reaction, UDP-Gal*p* or UDP-Gal*p*NAc (1 mM) was incubated with the appropriate mutase protein (3.9 μM) in 30 μl of 100 mM potassium phosphate buffer (pH 7.4) with freshly prepared sodium dithionite (20 mM) until equilibrium was reached as indicated by a constant product/substrate ratio by HPLC. The same procedure was used for the reverse reaction but instead using UDP-Gal*f* or UDP-Gal*f*NAc (1 mM) as the starting substrate.

Complementation of C. jejuni 11168 glf Knock-out—Shuttle plasmids (pWM1007/cat derivatives) expressing the *E. coli glf* and *C. jejuni glf* genes were mobilized into *C. jejuni* 11168 wild-type and the *glf* mutant as described (44). Capsular polysaccharides of the resulting strains were prepared as described (45) and visualized after 16.5% deoxycholate PAGE by silver staining using the protocol of Tsai and Frasch (46) with the modification that fixing was performed for only 2 h.

UGM Activity in E. coli—The *E. coli glf* mutant strain MFF1 (47) was transformed with plasmids containing *E. coli wbbL* (pMF19 (47)) and either empty vector pWM1007 or pWM1007 containing *glf* from *E. coli* or from *C. jejuni*. Strains were grown overnight after induction with 0.5 mM isopropyl β-D-1-thiogalactopyranoside. Lipopolysaccharides (LPS) were extracted following a modified protocol of Marolda *et al.* (48). Briefly, cells were adjusted to an absorbance of 3.0 (600 nm wavelength), resuspended in 150 μl of lysis buffer (2% SDS, 4% β-mercaptoethanol, 10% glycerol, 0.5 M Tris (pH 6.8)), and incubated at 100 °C for 10 min. After addition of 2 μl of proteinase K (20 mg/ml), samples were incubated for 2 h at 60 °C. To this solution was added 150 μl of hot phenol, and samples were incubated at 70 °C for 15 min, followed by 10 min on ice. After centrifugation, the aqueous phase was mixed with 250 μl of EtOH and centrifuged, and the precipitated LPS were dried at room temperature. LPS corresponding to an absorbance (A_{600}) of 0.45 were separated by SDS-PAGE, and LPS silver staining was performed according to Tsai and Frasch (46).

Homology Model of C. jejuni UNGM with Bound UDP-GalfNAc—A homology model of *C. jejuni* 11168 UNGM was generated based on the crystal structure of the *E. coli* UGM in the closed ring form (Protein Data Bank code 1I8T, chain A) (15) using ESyPred3D (49). Chain A was used as it has the mobile loop region in the active "closed" conformation. Using Autodock 4.0 (50), the UDP-Gal*p*NAc and UDP-Gal*f*NAc substrates were modeled into the active site. For each substrate, the low energy conformation, in which the nucleotide conformation agreed with the published crystal structure data of UGM bound to UDP-Glc*p* (28) and UDP-Gal*p* (29), was chosen to represent a plausible binding mode.

Mutagenesis of C. jejuni UNGM—The R59H, R168K, and R59H/R168K mutants were prepared using the QuikChange XL II protocol by Stratagene (51). In the case of the R59H and R168K, mutants were prepared from the pWM1007 plasmid containing the *glf* gene isolated from *E. coli* DH5α cells using *R59H_F* and *R59H_R* or *R168K_F* and *R168K_R* (supplemental Table S1) as primer pairs, respectively. In the case of R59H/R168K, the double mutant was prepared using the R59H

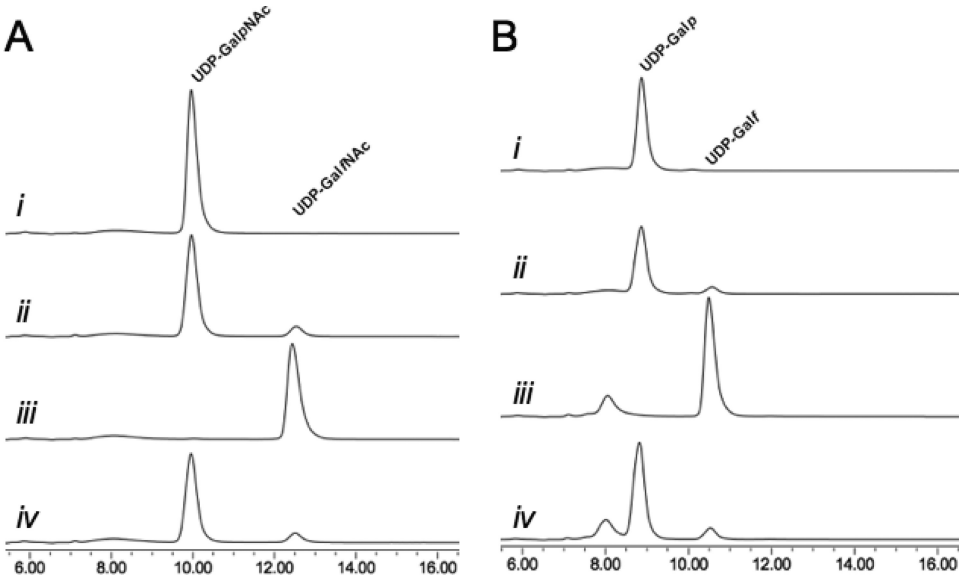

FIGURE 3. **Functional characterization of *C. jejuni* UNGM.** *A,* with UDP-GalNAc as the substrate. *Trace i,* retention time for a standard solution of UDP-Gal*p*NAc. *Trace ii,* incubation of UDP-Gal*p*NAc with *C. jejuni* UNGM at equilibrium. *Trace iii,* standard solution of the purified product (UDP-Gal*f*NAc) from the reaction of UDP-Gal*p*NAc with *C. jejuni* UNGM. *Trace iv,* incubation of UDP-Gal*f*NAc with *C. jejuni* UNGM at equilibrium. The same ratio of 93:7 UDP-Gal*p*NAc to UDP-Gal*f*NAc is seen as in *trace ii*. *B,* with UDP-Gal as the substrate. *Trace i,* retention time for a standard solution of UDP-Gal*p*. *Trace ii,* incubation of UDP-Gal*p* with UNGM at equilibrium. *Trace iii,* standard solution of UDP-Gal*f* produced enzymatically from Gal*f*-1-phosphate. *Trace iv,* incubation of UDP-Gal*f* with *C. jejuni* UNGM at equilibrium. The same ratio of 93:7 UDP-Gal*p* to UDP-Gal*f* seen in *trace ii* is also observed. The peak at ~8 min corresponds to UMP.

mutant pWM1007 plasmid and the *R168K_F* and *R168K_R* primer pair. After mutagenesis, the plasmid DNA was isolated from the XL10-gold cells and sequenced before being transformed into DH5α cells for protein expression.

Competitive Substrate Specificity Assay—A mixture of UDP-Gal*f* (0.5 mM) and UDP-Gal*f*NAc (0.5 mM) was incubated with the appropriate mutase protein (3.9 μM) in 100 mM potassium phosphate buffer (pH 7.4) containing freshly prepared sodium dithionite (20 mM) for 5 min. The reactions were again monitored using the same modified HPLC conditions of Zhang and Liu (16). In this case, the use of a lower concentration of acetonitrile (1.25%) and a flow rate of 0.6 ml/min allowed for better resolution of all four product and substrate peaks (UDP-Gal*p*, UDP-Gal*f*, UDP-Gal*p*NAc, and UDP-Gal*f*NAc). Using these conditions, these compounds were found to have retention times of 10.0, 12.4, 11.6, and 15.4 min, respectively. The relative specificity was determined by integration of the UDP-Gal*p* and UDP-Gal*p*NAc peaks.

Determination of UNGM and Mutant Kinetic Parameters—Kinetic parameters for wild-type *C. jejuni* UNGM and each of the mutants were determined following a kinetic assay modified from the procedure reported by Zhang and Liu (16). Reactions were prepared containing an appropriate concentration of the desired protein with UDP-Gal*f* or UDP-Gal*f*NAc (10, 12.5, 25, 50, 100, 250, and 500 μM) in a final volume of 60 μl of 100 mM potassium phosphate (pH 7.4) containing 20 mM of freshly prepared sodium dithionite. Incubations were carried out for 5 min at 37 °C and then promptly quenched by heating to 90 °C for 5 min. The sugar nucleotides do not decompose by loss of UDP under these quenching conditions, as evidenced by the lack of a peak in these HPLCs for UDP, which has a retention time of 11.2 min. The incubation mixtures were monitored by HPLC as described above. In all cases, a concentration of protein was used so that less than 40% conversion to the pyranose product was observed. The concentrations of UDP-Gal*p* or UDP-Gal*p*NAc were determined by integration of the appropriate peaks on the HPLC trace, and these were used to determine the initial velocities. Each assay was performed in duplicate for all proteins for each of the furanose substrates. The calculated enzyme specificity was determined using a modification of the Michaelis-Menten Equation 1 for two competing substrates (52),

$$\frac{v_A}{v_B} = \frac{(k_{cat}/K_M)_A[A]}{(k_{cat}/K_M)_B[B]} \quad \text{(Eq. 1)}$$

RESULTS

C. jejuni UNGM Functions as a UNGM in Vitro—When annotated, the *glf* gene product from *C. jejuni* 11168 was proposed to be a UGM based on homology (53), despite the lack of Gal*f* residues its glycoconjugates. Although it was later suggested that Glf may function in biosynthesis of Gal*f*NAc in the CPS (33), the function of the protein has never been examined. In this study, the purified *C. jejuni* UNGM was examined by incubation with UDP-Gal*p*NAc (compound 1) under the reducing conditions modified from Liu and Zhang (16), and conversion to products was monitored by reverse phase HPLC. Formation of a longer retention time product (12.5 min) was observed, and at equilibrium, a ratio of 7:93 with respect to the UDP-Gal*p*NAc peak resulted, as seen in Fig. 3*A* (*traces i* and *ii*). This reflects the equilibrium ratios observed for the *K. pneumoniae* (26) and *E. coli* (16) UGM with UDP-Gal. Scaling up the reaction gave access to sufficient quantities of the reaction product to characterize by ^{1}H NMR spectroscopy (Fig. 4*B*) and mass spectrometry. The observed mass was consistent with the product being UDP-Gal*f*NAc (compound 2), and the resonances in the ^{1}H NMR spectrum closely matched those previously reported for Gal*f*NAc residues in the CPS of *C. jejuni* 11168 (33) and the *O*-specific polysaccharide of *Proteus penneri* strain 22 (32). In particular, the characteristic coupling pattern for the Gal*f*NAc H-4 proton and the upfield shift of the H-5 proton confirmed a galactofuranose ring configuration (11). Incubation of the isolated product 2 with UNGM under the same reducing conditions gave, as expected, an equilibrium ratio of 7:93 UDP-Gal*f*NAc to UDP-Gal*p*NAc (Fig. 3*B*).

E. coli UGM Does Not Interconvert UDP-GalpNAc and UDP-GalfNAc—Earlier work established that the UGM of K. pneumoniae does not interconvert UDP-Gal*p*NAc and UDP-Gal*f*NAc (26), but no published data were available for the *E. coli* UGM. The *E. coli* UGM has a higher sequence identity,

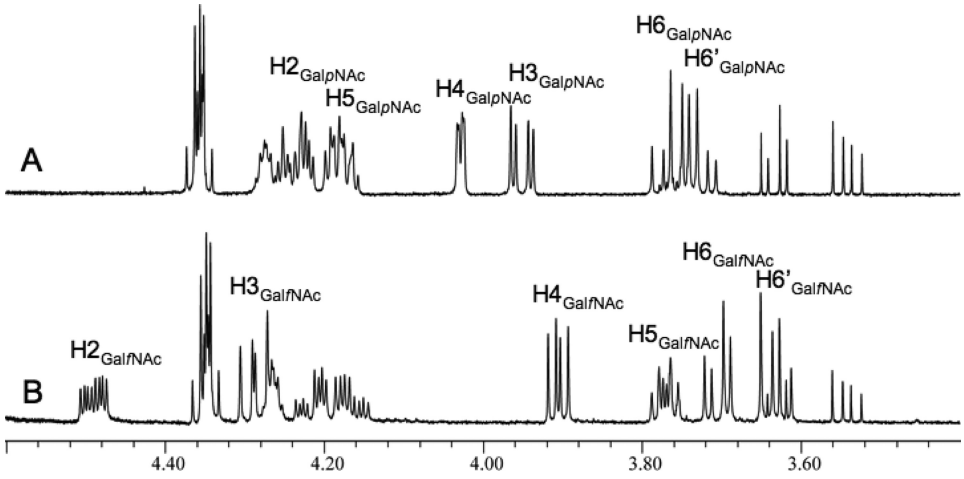

FIGURE 4. **^{1}H NMR analysis of the product of *C. jejuni* UNGM reaction with UDP-Gal*p*NAc.** *A,* region of the ^{1}H NMR spectrum of the starting material UDP-Gal*p*NAc. *B,* same region of the ^{1}H NMR spectrum for the UNGM reaction product. The observed chemical shifts and coupling constants are consistent for UDP-GalNAc in the furanose ring form.

TABLE 1
Kinetic parameters for the *C. jejuni* UNGM and mutants

Enzyme	Substrate	K_m	k_{cat}	k_{cat}/K_m	UDP-Gal: UDP-GalNAc
		μM	min^{-1}	$\mu M^{-1}\ min^{-1}$	
Wild type	UDP-Gal*f*	45 ± 3	178 ± 4	4.1	1.5
UNGM	UDP-Gal*f*NAc	40 ± 6	114 ± 5	2.8	
R59H	UDP-Gal*f*	92 ± 20	590 ± 50	6.4	15
	UDP-Gal*f*NAc	61 ± 7	26 ± 1	0.43	
R168K	UDP-Gal*f*	65 ± 9	96 ± 4	1.5	3.8
	UDP-Gal*f*NAc	231 ± 40	89 ± 7	0.39	
R59H/R168K	UDP-Gal*f*	77 ± 9	380 ± 20	4.9	21
	UDP-Gal*f*NAc	59 ± 6	13.8 ± 0.5	0.23	
E. coli UGM	UDP-Gal*f*NAc	ND[a]	ND[a]	ND[a]	ND[a]

[a] ND means none detected.

60%, with the *C. jejuni* 11168 UNGM than with the *K. pneumoniae* UGM (38% identity) with which it shares a function. Therefore, we wanted to determine whether the *E. coli* UGM recognized UDP-Gal*p*NAc as a substrate. We found that no conversion of UDP-Gal*p*NAc was detected using the *E. coli* UGM (Table 1), even upon prolonged incubations (60 min). A similar experiment, using UDP-Gal*f*NAc as the substrate, also demonstrated no conversion. To ensure that the protein was active, both UDP-Gal*p* and UDP-Gal*f* were used in the assay, and activity levels consistent with previously published results (16) were observed.

C. jejuni CPS Production Is Restored by Expressing the cj1439c Allele in Trans—To test the activity of the *glf*-His allele *in vivo*, the corresponding proteins were expressed in *trans* in *C. jejuni* wild-type and the *glf* mutant strain (Fig. 5*A*). CPS formation was followed by silver staining of crude CPS preparations. Expression of the Cj-*glf*-His allele resulted in restoration of CPS in the *cj1439c*(*glf*) mutant, whereas no CPS formation was observed upon expression of Ec-*glf*-His. The expression of an additional copy of Cj-*glf*-His, Ec-*glf*-His, or the presence of the empty plasmid (pWM1007/cat, negative control) in *C. jejuni* 11168 cells did not affect CPS formation.

C. jejuni UNGM Interconverts UDP-Galf and UDP-Galp in Vitro—The natural CPS of *C. jejuni* 11168 contains only Gal*f*NAc residues and no Gal*f* residues (33). To probe whether this observation is due to the specificity of the *C. jejuni* UNGM, the protein was incubated with both UDP-Gal*p* (compound 3) and UDP-Gal*f* (compound 4) (39). Interconversion between compounds 3 and 4 was observed in both cases (Fig. 3*B*). As was observed for compound 2, the equilibrium ratio was consistent with the 7:93 UDP-Gal*f* to UDP-Gal*p* ratio reported previously (16).

In a second experiment, co-incubation of UNGM with a 50:50 mixture of UDP-Gal*f* and UDP-Gal*f*NAc was carried out. This experiment was intended to provide an estimate of the relative specificity of the enzyme for these two substrates. At equilibrium, the ratio of the corresponding pyranose product was 2.48:1 in favor of UDP-Gal*p* as shown in Fig. 7.

C. jejuni UNGM Has UGM Activity in E. coli—Because the specificity of UNGM allows it to act as a UGM *in vitro*, we desired a method to test this activity in a cellular environment similar to the Δ*glf* complementation experiment in *C. jejuni.* Unfortunately, no *C. jejuni* serotypes containing Gal*f* residues have been identified. Conveniently, common *E. coli* laboratory strains such as W3110 are derived from serogroup O16, which contains Gal*f* as a component of the LPS O-antigen. In this species, the O-antigen is composed of a pentasaccharide repeating unit of (1→2)-β-D-Gal*f*-(1→6)-α-D-Glc*p*-(1→3)-α-L-Rha*p*-(1→3)-[(1→6)-α-D-Glc*p*]-α-D-Glc*p*NAc (47). The W3110 strain does not display a smooth LPS phenotype, due to an insertion sequence disrupting a gene encoding the rhamnosyltransferase (*wbbL*), which is required for the attachment of the second sugar of the O-antigen subunits. Re-introduction of the *wbbL* gene on a plasmid restores smooth LPS biosynthesis (54, 55). By mutating the *E. coli* O16 *glf* gene in a *wbbL*-complemented strain, only one incomplete *O* chain subunit, devoid of Gal*f*, is attached to the lipid A core (Fig. 5*B*, *lane 2*) (47). Wild-type LPS production is restored when *E. coli glf* is reintroduced (Fig. 5*B*, *lane 3*) (47). To prove *in vivo* UGM activity of the *C. jejuni* UNGM, we repeated the complementation of the *E. coli* Δ*glf* mutation using a plasmid carrying *C. jejuni glf*. As shown in the *4th lane* of Fig. 5*B*, the resulting strain produced full-length LPS, indicating that intact *O* chain subunits containing Gal*f* were synthesized and polymerized. Incorporation of Gal*f*NAc into the *O* chain can be ruled out because subunits of the O16 LPS are connected via an α-(1→2) linkage to Gal*f*, which would be prevented by the presence of an acetamido group at position 2, as in Gal*f*NAc. Furthermore, to the best of our knowledge, serogroup O16 *E. coli* strains do not produce UDP-Gal*p*NAc. Thus, the *E. coli* complementation studies indicate that *C. jejuni* UNGM can interconvert UDP-Gal*f* and UDP-Gal*p* *in vivo*.

Modeling the Active Site of UNGM Suggests the Origin of UDP-GalNAc Recognition—To investigate the origin of the increased substrate scope of *C. jejuni* UNGM compared with the highly homologous *E. coli* UGM, we examined differences

in the active site residues. No crystal structure for the *C. jejuni* UNGM has been determined; therefore, a homology model was generated based on the *E. coli* UGM for which a structure is available (15). After building the protein model, UDP-Gal*p*NAc (Fig. 6*A*) and UDP-Gal*f*NAc (Fig. 6*B*) were docked into the active site. Inspection of the resulting structure showed that the nucleotide portion was bound in a similar conformation to that observed in the crystal structure of *K. pneumoniae* UGM bound to UDP-Gal (28), which was recently reported. As was seen in the *K. pneumoniae* structure, a key base stacking interaction is predicted to occur with a tyrosine residue (Tyr-150).

Active site residues are highly conserved between the three bacterial UGM for which x-ray structures have been determined (*E. coli*, *K. pneumonia*, and *M. tuberculosis*) and the *C. jejuni* UNGM. Only one residue in the UNGM active site, arginine 59, differed from the conserved histidine found in all three bacterial UGMs (supplemental Fig. S2). A second residue, arginine 168 in UNGM, differs from the conserved lysine found in the *E. coli* and *K. pneumoniae* UGM. As seen in Fig. 6*A*, Arg-59 appears to be in close proximity to the carbonyl oxygen of the acetamido moiety of UDP-Gal*p*NAc. The other residue, Arg-168, is located adjacent to the conserved arginine, in this case Arg-169, in the mobile loop region that has previously been shown to be essential for UGM activity (20).

Mutagenesis of Arginines 59 and 168 Reduces the Ability of UNGM to Catalyze Interconversion of UDP-GalfNAc to UDP-GalpNAc—The two active site arginine residues, Arg-59 and -168, were examined for their role in the interconversion of UDP-Gal*f*NAc and UDP-Gal*p*NAc by UNGM. Site-directed mutagenesis was used to convert these residues to the corresponding amino acid from the *E. coli*/*K. pneumoniae* UGMs, *i.e.* arginine 59 to histidine and arginine 168 to lysine. The double mutant was also constructed with both R59H and R168K mutations. The specificity of the mutant UNGM was determined using a co-incubation assay with the same 50:50 mixture of UDP-Gal*f* and UDP-Gal*f*NAc. Again, the ratio of the corresponding pyranose products was used to determine the relative selectivity of each mutant for the two substrates (Fig. 7). The R59H mutation resulted in a decrease in the conversion of UDP-Gal*f*NAc and the selectivity for the corresponding substrate, whereas UDP-Gal*f* conversion increased by greater than 10-fold over the wild-type UNGM. The R168K mutation had a less pronounced effect causing only an approximate 2-fold increase in the selectivity for UDP-Gal*f* compared with the wild-type enzyme. Mutation of both residues R59H and R168K resulted in the largest decrease in the conversion of UDP-Gal*f*NAc to UDP-Gal*p*NAc and a selectivity increase for UDP-Gal*f* of greater than 12-fold in comparison to the wild-type UNGM.

Analysis of C. jejuni UNGM and Mutant Kinetics with UDP-Galf and UDP-GalfNAc Supports Results of the Co-incubation Assay—At equilibrium, the pyranose ring form is favored in the reaction of pyranose-furanose mutases. Therefore, substrate kinetics are often measured starting with the furanose form and monitoring the formation of the thermodynamically favored pyranose isomer (56). Thus, the kinetic parameters were determined for UNGM and each of the mutants using UDP-Gal*f*NAc and UDP-Gal*f*

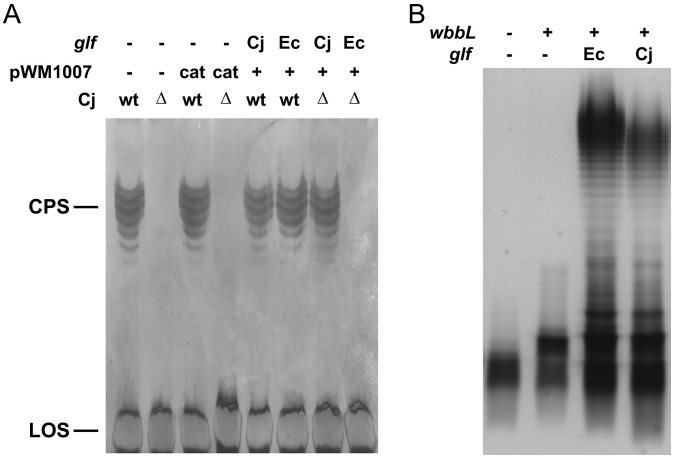

FIGURE 5. ***C. jejuni glf* gene complements CPS in *C. jejuni* Δ*glf* strain and LPS in *E. coli* Δ*glf* strain.** *A,* separation of *C. jejuni* 11168 crude CPS preparations by 16.5% deoxycholate PAGE. Equivalent amounts of sample were loaded in each lane that originated from bacterial cell cultures adjusted to an absorbance (A_{600}) of 3.0. Silver staining showed formation of CPS in the Cj-wt strain as well as Cj-wt with pMW1007/*cat*, pMW1007/Cj-*glf,* or pMW1007/Ec-*glf* plasmids. *wt* is wild type The *C. jejuni 1439c* (*glf*) knock-out strain (Cj-Δ) and the Cj-Δ strain with pMW1007/*cat* plasmid showed no CPS formation. Cj-Δ strain complemented with pMW1007/Cj-*glf* showed restoration of CPS production, and no CPS was observed in Cj-Δ complemented with pMW1007/Ec-*glf*. In all strains lipooligosaccharide (*LOS*) formation was not affected. *B,* LPS of *E. coli* strains derived from MFF1 were extracted after overnight growth and separated by SDS-PAGE. Equivalent amounts of sample were loaded in each lane that originated from bacterial cell cultures adjusted to an A_{600} of 0.45. Silver staining shows the production of a fast migrating band composed of lipid A core plus a GlcNAc residue (*wbbL* $^-$, *glf* $^-$); a band of higher molecular weight due to addition of an incomplete O antigen subunit to the lipid A core, which is only deficient of the Gal*f* residue (*wbbL* $^+$, *glf* $^-$); and smooth LPS when both *wbbL* and either the *E. coli* or the *C. jejuni glf* are present (*wbbL* $^+$, Ec-*glf* and *wbbL* $^+$, Cj-*glf*), respectively.

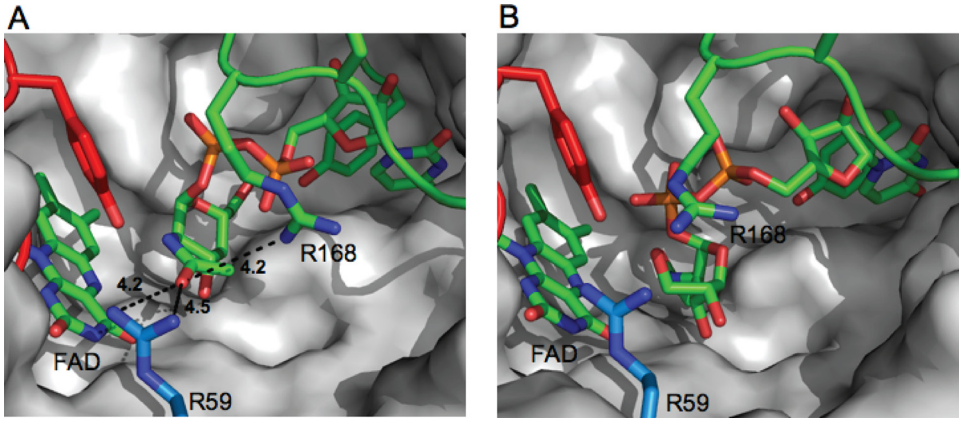

FIGURE 6. **Homology model of the active site of *C. jejuni* UNGM.** *A,* homology model of *C. jejuni* UNGM with the UDP-Gal*p*NAc substrate docked. The UDP-Gal*p*NAc appears to be bound in an active conformation with the Gal*p*NAc C-1 located in proximity to the FADH$^-$ cofactor. UDP is positioned similar to that in the crystal structure of *K. pneumoniae* bound to UDP-Glc by Kiessling and co-workers (28). Nonconserved active site residues Arg-59 and Arg-168 and their distance from the acetamido carbonyl oxygen are highlighted. *B,* homology model of *C. jejuni* UNGM with the UDP-Gal*f*NAc substrate bound. The UDP-Gal*f*NAc appear bound in an inactive conformation (no possible interaction between Gal*f*NAc C-1 and FADH$^-$ cofactor). Nonconserved active site residues Arg-59 and Arg-168 are highlighted.

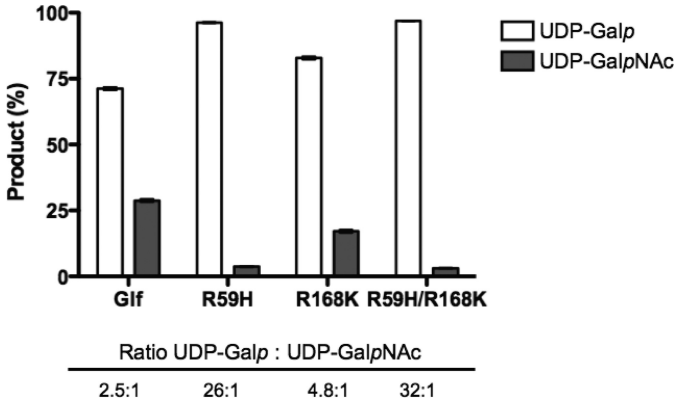

FIGURE 7. **Co-incubation assay of *C. jejuni* UNGM with 50:50 UDP-Gal*f*NAc and UDP-Gal*f*.** After co-incubation, the relative amounts of UDP-Gal*p* and UDP-Gal*p*NAc were determined based on the total amount of products observed. Shown are the average of three co-incubation assays for each of the *C. jejuni* UNGM and the R59H, R168K, and R59H/R168K UNGM mutants. Also shown is the specificity of the protein represented by the ratio of UDP-Gal*p* to UDP-Gal*p*NAc.

as substrates. As seen in Table 1, the K_m value of wild-type UNGM is approximately the same for both UDP-Gal*f* and UDP-Gal*f*NAc; however, the k_{cat} value is larger for UDP-Gal*f*. The R59H mutant showed only small changes in the K_m value for both substrates as compared with the wild-type UNGM. At the same time, there is a significant decrease in k_{cat} values observed for UDP-Gal*f*NAc in addition to an increase in the k_{cat} values for UDP-Gal*f*. Conversely, the R168K mutant displayed approximately the same k_{cat} value for both substrates, but the K_m value was significantly larger for UDP-Gal*f*NAc as the substrate. For each protein, the first-order rate constants were approximated by calculating k_{cat}/K_m values for each substrate (Table 1). The ratio of the first-order rate constants for UDP-Gal*f* over UDP-Gal*f*NAc could be used to approximate the specificity of each protein for UDP-Gal*f* as the incubation times for each substrate remained constant (52). The calculated specificities in each case mirror those determined using the co-incubation assay (Fig. 7), but the former approach underestimates these differences.

DISCUSSION

In this paper, we have tested a previously proposed hypothesis (57) that the *C. jejuni* 11168 gene *cj1439* encodes a protein responsible for the biosynthesis of the UDP-Gal*f*NAc. Our investigations have shown that, unlike the highly homologous UGM from *E. coli* and *K. pneumoniae*, the *C. jejuni* enzyme is able to convert the sugar nucleotide UDP-Gal*p*NAc to UDP-Gal*f*NAc, the precursor of Gal*f*NAc in the CPS. Thus, the protein is a UNGM. In addition, we have demonstrated that the *C. jejuni* UNGM also converts UDP-Gal*p* to UDP-Gal*f* both *in vitro* and *in vivo* in *E. coli*. We also identified two amino acids in the active site of UNGM that play a role in the interconversion of UDP-Gal*f*NAc and UDP-Gal*p*NAc. Our co-incubation assay allowed us to examine, in a single reaction, the substrate specificity of wild-type UNGM protein and each of the UNGM mutants.

Cj1439 Encodes for a Protein with Both UGM and UNGM Activity—This study represents the first demonstration of an enzyme involved in the interconversion of UDP-Gal*p*NAc and UDP-Gal*f*NAc. This enzyme, which bears a high sequence similarity to known UGMs, produces UDP-Gal*f*NAc from UDP-Gal*p*NAc presumably via a similar ring contraction mechanism. Both *in vitro* investigations and an *in vivo* complementation experiment support the role of UNGM in the biosynthesis of the Gal*f*NAc in *C. jejuni* 11168. In addition, we have demonstrated that the *C. jejuni* UNGM has dual substrate specificity and can interconvert the furanose and pyranose isomers of both UDP-Gal and UDP-GalNAc. Furthermore, the UGM activity of the *C. jejuni* enzyme has been demonstrated *in vivo* where it is able to complement the activity of the *E. coli* UGM in a *glf* gene knock-out.

It is not unusual that bacteria with compact genomes express enzymes that exhibit more than one activity. These bifunctional enzymes are widespread among bacteria and allow for the synthesis of many complex structures advantageous to the survival of the organism while still maintaining a small genome size. An example is the *wbbO* gene product from *K. pneumoniae*, a galactosyltransferase that catalyzes the transfer of both Gal*p* and Gal*f* residues in the biosynthesis of the lipopolysaccharide O1 antigen (58). Bifunctional enzymes have also been characterized in *C. jejuni*. For example, a single UDP-GlcNAc/Glc 4-epimerase was shown to be involved in the biosynthesis of three cell surface glycoconjugates in strain 11168 (59). Because the CPS structures in *C. jejuni* are highly variable between serotypes, it is reasonable to hypothesize that a bifunctional UNGM would be advantageous. However, no Gal*f* residues have been identified in any glycoconjugate from this organism. Thus, the inclusion of Gal*f*NAc, instead of Gal*f*, into the CPS appears to be due to the specificity of the cognate glycosyltransferase.

Comparing Calculated Specificity of C. jejuni UNGM to the Experimentally Determined Specificity—In this study, two methods were used to determine the substrate specificity of the *C. jejuni* UNGM. The first was the direct determination from the ratio of product conversion observed in the co-incubation assay (Fig. 7). The second was calculated using the observed kinetic parameters for each protein with UDP-Gal*f* or UDP-Gal*f*NAc (Table 1). The observed trend of substrate specificity is the same by either method; however, the calculated specificity in each case is lower than that determined using the co-incubation assay. The calculated substrate specificity may not accurately represent the observed specificity as the combined rate of the two competing reactions may be greater than, equal to, or lower than the rate of each individual reaction (60). Because of this, it appears that the co-incubation assay more accurately represents the substrate specificity of the UNGM for its two competing substrates UDP-Gal*f* and UDP-Gal*f*NAc.

Effect of Two Active Site Arginines on UDP-GalNAc Recognition by UNGM—We believed that residues in, or in proximity to, the active site would play a role in the different substrate specificity of the *C. jejuni* UNGM compared with other known UGM enzymes. We also rationalized that these key residues would be conserved in the other UGM but not in the *C. jejuni* enzyme. The only two residues that fit these criteria were Arg-59 and Arg-168. In both cases, these residues were found to be other basic amino acids, histidine and lysine, respectively, in the *E. coli* and *K. pneumoniae* UGM. In *M. tuberculosis,* Arg-59 was also replaced by histidine; however, Arg-168 was found to

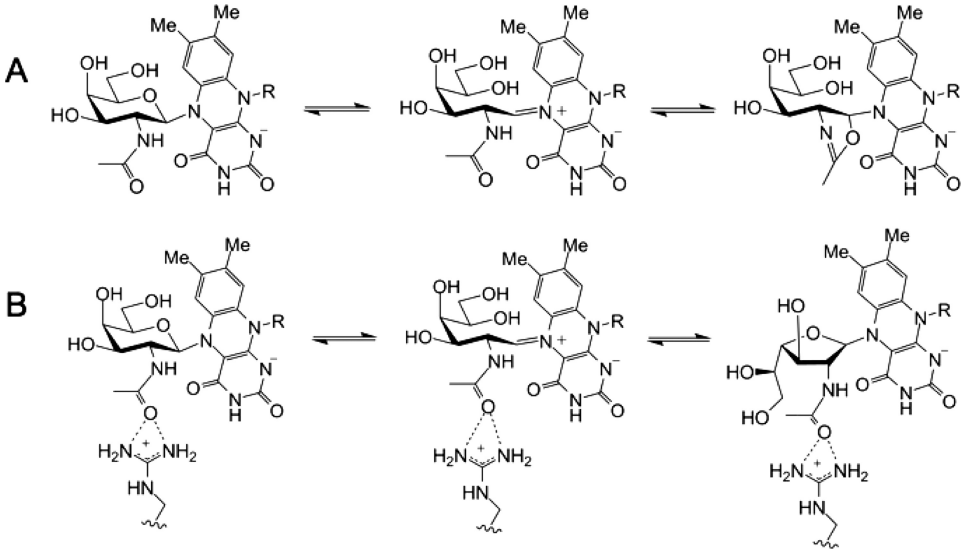

FIGURE 8. **Formation of oxazoline intermediate.** *A,* acetamido group of GalNAc can undergo an unproductive intramolecular reaction to form an FAD-bound oxazoline intermediate that prevents conversion to Gal*f*NAc. *B,* possible interaction between Arg-59 and the GalNAc acetamido group that would prevent formation of an oxazoline intermediate and promote conversion to Gal*f*NAc.

be a threonine rather than the lysine observed in *E. coli* and *K. pneumoniae*.

Mutagenesis of R168K only resulted in a 2-fold increase in selectivity for UDP-Gal*f* over UDP-Gal*f*NAc in the co-incubation assay; however, there were more significant changes observed for the kinetic parameters. This amino acid change resulted in a decrease in the catalytic activity of the protein for both substrates compared with the wild-type UNGM, but most interesting was that this substitution resulted in a significant increase in the K_m value with UDP-Gal*f*NAc but not with UDP-Gal*f*. As the K_m value approximates the dissociation constant for the enzyme-substrate complex, this supports the notion that Arg-168 has a role in binding and stabilizing UDP-GalNAc in the active site. It has previously been proposed that amino acid residues in the mobile loop of UGMs are involved in substrate recognition (19, 20). As Arg-168 is located in the mobile loop, its ability to stabilize the UDP-GalNAc enzyme-substrate complex is consistent with the role of the mobile loop in substrate recognition. This arginine residue is located 4.2 Å from the acetamido carbonyl oxygen in our homology model with docked UDP-Gal*p*NAc (Fig. 6*A*), indicating a possible hydrogen bonding interaction.

Mutation of the other active site arginine (Arg-59) indicates that it also plays an important role in the catalytic activity of UNGM. Mutagenesis of R59H results in a greater than 4-fold decrease in k_{cat} for UDP-Gal*f*NAc, while simultaneously resulting in a 3-fold increase in k_{cat} for UDP-Gal*f*. The K_m value is also changed for both substrates, but this appears minor in comparison with the observed changes in k_{cat}. Considering our homology model, Arg-59 is located within 4.5 Å of the carbonyl oxygen of the acetamido group of UDP-Gal*p*NAc (Fig. 6*A*). In the *E. coli* UGM crystal structure, the equivalent residue His-59 sits below the active site (data not shown) and does not protrude into the active site as does Arg-59 in UNGM. Therefore, it appears that Arg-59 is able to interact with the UDP-GalNAc substrate to stabilize the intermediate. This may occur by preventing the formation of nonproductive oxazoline-like intermediates, which could be formed by an intramolecular reaction of the acetamido group (Fig. 8). When the substrate is UDP-Gal, then there is no possibility of forming such intermediates. Therefore, Arg-59 does not aid in catalysis. Instead, because arginine is more bulky than histidine, it could lower the catalytic rate due to steric interactions in the active site during catalysis.

The mutagenesis of both R59H and R168K results in a larger decrease in turnover of UDP-Gal*f*NAc substrate while simultaneously increasing turnover of UDP-Gal*f*. This results in an increased selectivity for UDP-Gal*f* than observed for either of the single mutants (Fig. 7; Table 1). Somewhat surprisingly, the increase in the K_m value for UDP-Gal*f*NAc seen for the R168K mutant was not observed in the case of the double mutant. This suggests that the amino acids play a synergistic role in allowing the enzyme to interconvert UDP-Gal*f*NAc and UDP-Gal*p*NAc, rather than an additive role in which Arg-59 is the major determinant.

Subtle Amino Acid Substitutions Result in Changes in C. jejuni UNGM Substrate Tolerance—Despite the high sequence identity of *C. jejuni* UNGM with the *E. coli*, *M. tuberculosis,* and *K. pneumoniae* UGM, the UNGM possesses the ability to recognize UDP-GalNAc as a substrate. Most of the sequence variability occurs in solvent-exposed residues, and the amino acids making up the active site are nearly identical in all four mutase enzymes (supplemental Fig. S2, *boxed residues*). The two residues identified here as playing an important role in allowing recognition of UDP-GalNAc are relatively conservative replacements of the residues found in the other mutase enzymes; however, they nevertheless have a significant effect on the substrate selectivity of the enzyme. It should be appreciated that small variations in amino acids leading to changes in substrate specificity are well known in carbohydrate-active enzymes. For example, the blood group GTA and GTB glycosyltransferases, which use UDP-Gal*p*NAc *versus* UDP-Gal*p*, respectively, as the donor substrate, differ in only four amino acids (61). Similarly, in *Neisseria meningitidis*, a single amino acid change in the capsule polymerase determines the substrate specificity for either Glc*p* or Gal*p* transferase activity (62).

Although the two arginine residues identified in this study influence the substrate specificity, the mutagenesis of either residue or both failed to result in a complete loss in UNGM activity. It is therefore clear that other amino acids further removed from the active site also contribute to the specificity of the enzyme, and these remain to be elucidated. As well, we have demonstrated that *C. jejuni* UNGM can function as a UGM *in vivo*; however, there have been no Gal*f* residues reported in *C. jejuni* glycoconjugates. In this context, another unresolved issue is if other *C. jejuni* strains

containing the *glf* gene possess Gal*f*-containing glycoconjugates, and investigations into the specificity of the transferases accepting donors from bifunctional enzymes are warranted. This study further demonstrates the intricacies in bacterial glycoconjugate biosynthesis. Detailed understanding of these systems will allow for the development of novel antimicrobials targeting these pathogen-specific pathways.

REFERENCES

1. Peltier, P., Euzen, R., Daniellou, R., Nugier-Chauvin, C., and Ferrières, V. (2008) *Carbohydr. Res.* **343,** 1897–1923
2. Richards, M. R., and Lowary, T. L. (2009) *ChemBioChem* **10,** 1920–1938
3. de Lederkremer, R. M., and Colli, W. (1995) *Glycobiology* **5,** 547–552
4. Whitfield, C. (1995) *Trends Microbiol.* **3,** 178–185
5. Brennan, P. J., and Nikaido, H. (1995) *Annu. Rev. Biochem.* **64,** 29–63
6. Lee, R. E., Smith, M. D., Nash, R. J., Griffiths, R. C., McNeil, M., Grewal, R. K., Yan, W. X., Besra, G. S., Brennan, P. J., and Fleet, G. W. (1997) *Tetrahedron Lett.* **38,** 6733–6736
7. Pan, F., Jackson, M., Ma, Y., and McNeil, M. (2001) *J. Bacteriol.* **183,** 3991–3998
8. Pedersen, L. L., and Turco, S. J. (2003) *Cell. Mol. Life Sci.* **60,** 259–266
9. Belánová, M., Dianisková, P., Brennan, P. J., Completo, G. C., Rose, N. L., Lowary, T. L., and Mikusová, K. (2008) *J. Bacteriol.* **190,** 1141–1145
10. Nassau, P. M., Martin, S. L., Brown, R. E., Weston, A., Monsey, D., McNeil, M. R., and Duncan, K. (1996) *J. Bacteriol.* **178,** 1047–1052
11. Köplin, R., Brisson, J. R., and Whitfield, C. (1997) *J. Biol. Chem.* **272,** 4121–4128
12. Weston, A., Stern, R. J., Lee, R. E., Nassau, P. M., Monsey, D., Martin, S. L., Scherman, M. S., Besra, G. S., Duncan, K., and McNeil, M. R. (1997) *Tuber Lung Dis.* **78,** 123–131
13. Beverley, S. M., Owens, K. L., Showalter, M., Griffith, C. L., Doering, T. L., Jones, V. C., and McNeil, M. R. (2005) *Eukaryotic Cell* **4,** 1147–1154
14. Bakker, H., Kleczka, B., Gerardy-Schahn, R., and Routier, F. H. (2005) *Biol. Chem.* **386,** 657–661
15. Sanders, D. A., Staines, A. G., McMahon, S. A., McNeil, M. R., Whitfield, C., and Naismith, J. H. (2001) *Nat. Struct. Biol.* **8,** 858–863
16. Zhang, Q., and Liu, H. (2000) *J. Am. Chem. Soc.* **122,** 9065–9070
17. Soltero-Higgin, M., Carlson, E. E., Gruber, T. D., and Kiessling, L. L. (2004) *Nat. Struct. Mol. Biol.* **11,** 539–543
18. Beis, K., Srikannathasan, V., Liu, H., Fullerton, S. W., Bamford, V. A., Sanders, D. A., Whitfield, C., McNeil, M. R., and Naismith, J. H. (2005) *J. Mol. Biol.* **348,** 971–982
19. Yao, X. H., Bleile, D. W., Yuan, Y., Chao, J., Sarathy, K. P., Sanders, D. A., Pinto, B. M., and O'Neill, M. A. (2009) *Proteins Struct. Funct. Bioinformat.* **74,** 972–979
20. Chad, J. M., Sarathy, K. P., Gruber, T. D., Addala, E., Kiessling, L. L., and Sanders, D. A. R. (2007) *Biochemistry* **46,** 6723–6732
21. Caravano, A., Sinaÿ, P., and Vincent, S. P. (2006) *Bioorg. Med. Chem. Lett.* **16,** 1123–1125
22. Itoh, K., Huang, Z., and Liu, H. W. (2007) *Org. Lett.* **9,** 879–882
23. Carlson, E. E., May, J. F., and Kiessling, L. L. (2006) *Chem. Biol.* **13,** 825–837
24. Zhang, Q., and Liu, H. (2001) *J. Am. Chem. Soc.* **123,** 6756–6766
25. Yuan, Y., Bleile, D. W., Wen, X., Sanders, D. A., Itoh, K., Liu, H. W., and Pinto, B. M. (2008) *J. Am. Chem. Soc.* **130,** 3157–3168
26. Errey, J. C., Mann, M. C., Fairhurst, S. A., Hill, L., McNeil, M. R., Naismith, J. H., Percy, J. M., Whitfield, C., and Field, R. A. (2009) *Org. Biomol. Chem.* **7,** 1009–1016
27. Yuan, Y., Wen, X., Sanders, D. A., and Pinto, B. M. (2005) *Biochemistry* **44,** 14080–14089
28. Gruber, T. D., Borrok, M. J., Westler, W. M., Forest, K. T., and Kiessling, L. L. (2009) *J. Mol. Biol.* **391,** 327–340
29. Gruber, T. D., Westler, W. M., Kiessling, L. L., and Forest, K. T. (2009) *Biochemistry* **48,** 9171–9173
30. Feng, L., Senchenkova, S. N., Yang, J., Shashkov, A. S., Tao, J., Guo, H., Cheng, J., Ren, Y., Knirel, Y. A., Reeves, P. R., and Wang, L. (2004) *J. Bacteriol.* **186,** 4510–4519
31. Hanniffy, O. M., Shashkov, A. S., Moran, A. P., Prendergast, M. M., Senchenkova, S. N., Knirel, Y. A., and Savage, A. V. (1999) *Carbohydr. Res.* **319,** 124–132
32. Arbatsky, N. P., Shashkov, A. S., Mamyan, S. S., Knirel, Y. A., Zych, K., and Sidorczyk, Z. (1998) *Carbohydr. Res.* **310,** 85–90
33. St Michael, F., Szymanski, C. M., Li, J., Chan, K. H., Khieu, N. H., Larocque, S., Wakarchuk, W. W., Brisson, J. R., and Monteiro, M. A. (2002) *Eur. J. Biochem.* **269,** 5119–5136
34. Eppe, G., Peltier, P., Daniellou, R., Nugier-Chauvin, C., Ferrières, V., and Vincent, S. P. (2009) *Bioorg. Med. Chem. Lett.* **19,** 814–816
35. Wang, Q., Ding, P., Perepelov, A. V., Xu, Y., Wang, Y., Knirel, Y. A., Wang, L., and Feng, L. (2008) *Mol. Microbiol.* **70,** 1358–1367
36. Allos, B. M. (2001) *Clin. Infect. Dis.* **32,** 1201–1206
37. Kaldor, J., and Speed, B. R. (1984) *Br. Med. J.* **288,** 1867–1870
38. Delederkremer, R. M., Nahmad, V. B., and Varela, O. (1994) *J. Org. Chem.* **59,** 690–692
39. Errey, J. C., Mukhopadhyay, B., Kartha, K. P., and Field, R. A. (2004) *Chem. Commun.* 2706–2707
40. Miller, W. G., Bates, A. H., Horn, S. T., Brandl, M. T., Wachtel, M. R., and Mandrell, R. E. (2000) *Appl. Environ. Microbiol.* **66,** 5426–5436
41. Marolda, C. L., Welsh, J., Dafoe, L., and Valvano, M. A. (1990) *J. Bacteriol.* **172,** 3590–3599
42. Carrillo, C. D., Taboada, E., Nash, J. H., Lanthier, P., Kelly, J., Lau, P. C., Verhulp, R., Mykytczuk, O., Sy, J., Findlay, W. A., Amoako, K., Gomis, S., Willson, P., Austin, J. W., Potter, A., Babiuk, L., Allan, B., and Szymanski, C. M. (2004) *J. Biol. Chem.* **279,** 20327–20338
43. Yao, R., Alm, R. A., Trust, T. J., and Guerry, P. (1993) *Gene* **130,** 127–130
44. Nothaft, H., Liu, X., McNally, D. J., Li, J., and Szymanski, C. M. (2009) *Proc. Natl. Acad. Sci. U.S.A.* **106,** 15019–15024
45. Bacon, D. J., Szymanski, C. M., Burr, D. H., Silver, R. P., Alm, R. A., and Guerry, P. (2001) *Mol. Microbiol.* **40,** 769–777
46. Tsai, C. M., and Frasch, C. E. (1982) *Anal. Biochem.* **119,** 115–119
47. Feldman, M. F., Marolda, C. L., Monteiro, M. A., Perry, M. B., Parodi, A. J., and Valvano, M. A. (1999) *J. Biol. Chem.* **274,** 35129–35138
48. Marolda, C. L., Lahiry, P., Vinés, E., Saldías, S., and Valvano, M. A. (2006) *Methods Mol. Biol.* **347,** 237–252
49. Lambert, C., Léonard, N., De Bolle, X., and Depiereux, E. (2002) *Bioinformatics* **18,** 1250–1256
50. Morris, G. M., Goodsell, D. S., Halliday, R. S., Huey, R., Hart, W. E., Belew, R. K., and Olson, A. J. (1998) *J. Comput. Chem.* **19,** 1639–1662
51. Bian, X. L., Rosas-Acosta, G., Wu, Y. C., and Wilson, V. G. (2007) *J. Virol.* **81,** 2899–2908
52. Fersht, A. (1999) in *Structure and Mechanism in Protein Science: A Guide to Enzyme Catalysis and Protein Folding* (Julet, M. R., ed) pp. 116–117, W. H. Freeman & Co., New York
53. Parkhill, J., Wren, B. W., Mungall, K., Ketley, J. M., Churcher, C., Basham, D., Chillingworth, T., Davies, R. M., Feltwell, T., Holroyd, S., Jagels, K., Karlyshev, A. V., Moule, S., Pallen, M. J., Penn, C. W., Quail, M. A., Rajandream, M. A., Rutherford, K. M., van Vliet, A. H., Whitehead, S., and Barrell, B. G. (2000) *Nature* **403,** 665–668
54. Liu, D., and Reeves, P. R. (1994) *Microbiology* **140,** 49–57
55. Stevenson, G., Neal, B., Liu, D., Hobbs, M., Packer, N. H., Batley, M., Redmond, J. W., Lindquist, L., and Reeves, P. (1994) *J. Bacteriol.* **176,** 4144–4156
56. Lee, R., Monsey, D., Weston, A., Duncan, K., Rithner, C., and McNeil, M. (1996) *Anal. Biochem.* **242,** 1–7
57. Karlyshev, A. V., Champion, O. L., Churcher, C., Brisson, J. R., Jarrell, H. C., Gilbert, M., Brochu, D., St Michael, F., Li, J., Wakarchuk, W. W., Goodhead, I., Sanders, M., Stevens, K., White, B., Parkhill, J., Wren, B. W., and Szymanski, C. M. (2005) *Mol. Microbiol.* **55,** 90–103
58. Guan, S., Clarke, A. J., and Whitfield, C. (2001) *J. Bacteriol.* **183,** 3318–3327
59. Bernatchez, S., Szymanski, C. M., Ishiyama, N., Li, J., Jarrell, H. C., Lau, P. C., Berghuis, A. M., Young, N. M., and Wakarchuk, W. W. (2005) *J. Biol. Chem.* **280,** 4792–4802
60. Cha, S. (1968) *Mol. Pharmacol.* **4,** 621–629
61. Rose, N. L., Palcic, M. M., and Evans, S. V. (2005) *J. Chem. Educ.* **82,** 1846–1852
62. Claus, H., Stummeyer, K., Batzilla, J., Mühlenhoff, M., and Vogel, U. (2009) *Mol. Microbiol.* **71,** 960–971